Proof of Concept: Electrical Stimulation Waveform Control by Closed-Loop Regulation by Means of Impedance Spectra Monitoring

F. Dupont, C. Condemine, J-F. Bêche, P. Pham, M. Belleville

CEA-Leti, MINATEC campus, 17 rue des Martyrs, 38054 Grenoble Cedex 9, France

Abstract

While neuroscientists need to control the signal transmitted to the stimulation targets to perform relevant electrophysiological analysis, the electrode-tissue impedance acts as a filter. Consequently, electrical stimuli must be adapted to this impedance. In this paper, a new strategy is proposed to control the stimulus waveform at the stimulation target proximity. Electrochemical Impedance Spectroscopy monitoring data are processed and a closed-loop system allows the generation of adapted waveforms. The proof of concept is tested on Equivalent Electrical Circuit models for two applications: Deep Brain Stimulation and Retinal Stimulation. Experimental results confirm the stimuli processing platform functionality. The method application range is discussed at the end of this paper.

Keywords*: Electrical Stimulation, Impedance Monitoring, Electrode-Tissue Interface, Closed-Loop, Waveform.*

Introduction

Neurons communicate between each other using electrical signals. Electrical stimulation allows modifying cells local electrical environment to trigger, inhibit or modulate their activity. Consequently, electrical stimulation addresses many neural disorders [1] thanks to dedicated techniques such as Parkinson disease with Deep Brain Stimulation (DBS), epilepsy with Vagus Nerve Stimulation (VNS) or Age-related Macular Degeneration (AMD) with Retinal Stimulation (RS). However, stimulation mechanisms being still poorly understood [2], the question about the stimulation patterns efficiency is asked by neuroscientists.

Stimulators and especially implantable devices face two main issues: the optimization of power needed for stimulation in order to increase the life-span of implanted systems and the stimuli effective waveform control at the stimulation targets vicinity. In voltage-mode stimulations, voltage stimuli are filtered by the equivalent electrode-tissue system electrical impedance [3]. In current-mode stimulations, the eventual shaping comes from voltage output stage saturation [3]. Moreover, trends lead to increase electrode integration density and thus to reduce electrode size. Higher impedance levels will then appear at the interface, increasing saturation risks. To address this latter issue, Ethier et al [4] designed a dual-chip current-mode stimulator where the second stage integrates a charge pump increasing thus the voltage output swing. This technique is performed in exchange of die area loss and additional costs. From these statements, we conclude that the effective signal delivered to stimulation targets is likely not the one generated by the implanted device. Consequently, electrical stimuli must be adapted to the electrode-tissue impedance in order to ensure electrophysiological interpretations' accuracy.

To quantify the impedance, fits are performed with Equivalent Electrical Circuits (EEC) on *in vivo* measured impedance spectral data. *In vivo* impedance varies with stimulus characteristics (magnitude, frequency), electrode configuration (size, layout), tissue properties and electrode-tissue interface temporal modifications (fibrosis, glial tissue …) [4]. As a consequence, electrode-tissue impedance monitoring is mandatory for preserving stimulus adaptation relevance. The aim of this monitoring is to predict the stimulus shaping and to generate a controlled signal at the target site. Based on a skin impedance measurement campaign, Johnson et al [5] proposed a dedicated voltage pattern for transcutaneous electrical neuromuscular stimulation. Even based on prior external impedance spectral analysis, this solution might be inadequate considering electrode-tissue impedance variations along the implant's life.

Our study introduces the proof of concept of temporal effective waveform control at the stimulation target proximity. It carries out a voltage-mode stimulation platform with the capability to deliver a controlled voltage pattern to

the stimulation targets taking into account the electrode-tissue interface shaping. This electrophysiological setup has been tested onto EEC models for *in vivo* retina and deep brain impedances.

Materials and Methods

The Stimuli Processing Platform

The stimuli processing platform's (Fig. 1) architecture is: an *Electrochemical Impedance Spectroscopy* (EIS) module, an *Identification Algorithm* module fitting EIS data to an EEC, a *Transfer Function Computing* module and a *Closed-Loop Algorithm* module computing adapted stimuli emitted by the *Stimuli Generator* module.

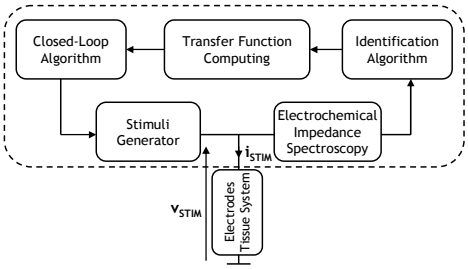

Fig. 1: Stimuli processing platform architecture.

Furthermore, this platform will be integrated in an ASIC (Application Specific Integrated Circuit) with external processing modules. In this study, the platform is carried out with commercial devices.

EIS measurements are performed with a Bio-Logic potentiostat (VMP2 type). Data are fitted to chosen EEC using the associated software (EC-Lab). Fig. 2 presents EIS results for *in vivo* DBS (monkey hippocampal region) and RS (rat subretinal region) measurements (circle markers). For each spectrum, fits based on two different complexity level EECs (see Fig. 3), are plotted in the graph (solid and dashed lines).

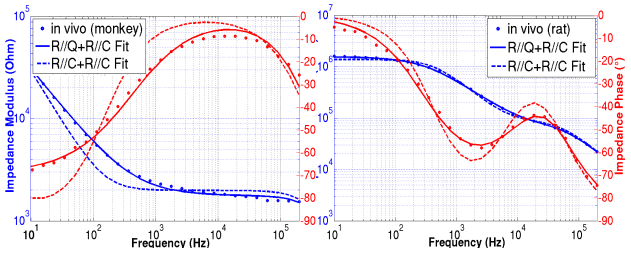

Fig. 2: EIS data (20mVpp) and corresponding EEC fit plots for *in vivo* DBS (left) and *in vivo* RS (right). Modulus is in blue and phase is in red. EECs appearing in the legend are detailed in Fig. 3.

The DBS electrode (DIXI Microdeep D08) has five 2mm² cylindrical Platinum contacts. It was implanted at the Grenoble Institute of Neuroscience (GIN). The RS electrode is a MicroElectrode Array (MEA) with nine 250µm² circular Platinum contacts. It was manufactured at the CEA-Leti and implanted in rat retinas at the Institut des Neurosciences de la Timone (INT). The experimental protocol had been previously approved by the local Ethical Committee for Animal Research and all procedures complied with the French and European regulations for Animal Research.

To get the most relevant fit, EEC elements are chosen as physicochemical phenomenon representative models [6]. They can be described by different model levels. Most accurate fits should require non-linear EEC elements toward signal magnitude and frequency but such elements are not available [7] (see *Discussion*). However, dedicated fitting EEC elements such as a Constant Phase Element (CPE or $Q_{interface}$) might be used to obtain an accurate fit of the electrode-tissue interface [8]. Considering CPE electronic implementation difficulties [9], an "approximated" EEC model based on linear elements (resistor and capacitor) can be used implying a fit quality drop-off visible on Fig. 2 (dashed lines).

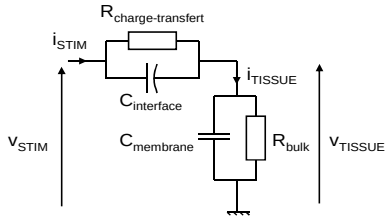

Fig. 3: Equivalent Electrical Circuit (EEC) modelling the measured electrode-tissue electrical impedance. Replacing $C_{interface}$ by $Q_{interface}$ provides a more accurate fit on data (see Fig. 2, solid lines).

Linear EEC of Fig. 3 is used for the proof of concept of this study. Nevertheless, the stimuli processing platform implementation will be able to perform stimuli adaptation irrespective of the chosen EEC model level.

A transfer function (H) linking V_{STIM} or I_{STIM} to V_{TISSUE} or I_{TISSUE}. Thus, four different signal pairs can be chosen depending on the chosen stimulator mode and the chosen signal to control. It means that four different expressions of H may be used.

Finally, to compute the adapted signal to be generated by the stimuli generator, one solution is the inverse transfer function H^{-1} estimation. However, both impedance non linearities [7], [8] (see Fig. 7 and the *Discussion* section) and different noise sources (biological and electronic origin) prevent from using basic inversion methods.

To address this issue, we carried out a control theory method called a close-loop system (Fig. 4). Its purpose is to minimize the error ε(t) between the variable set point $S_{DEF\_TISSUE}(t)$ and the feedback signal $S_{TISSUE}(t)$. As a consequence, the

adapted output signal $S_{STIM}(t)$ is computed during $S_{DEF\_TISSUE}(t)$ online tracking. This solution completely bypasses the necessity to compute H^{-1}.

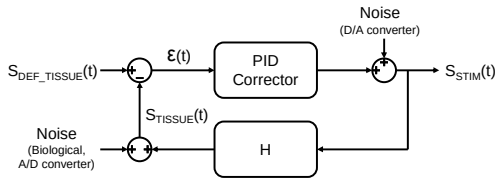

Fig. 4: Closed-loop system using a PID controller.

Feedback controllers have already been used in Functional Electrical Stimulation for example in muscle motion servo loop [10]. The classic PID controller linear transfer function is:

$$Corr(s) = K_P\left(1 + \frac{1}{sT_I} + sT_D\right) \quad (2)$$

where K_P, T_I and T_D are the PID tunable coefficients. The coefficients choice depends on control theory techniques [10].

The stimuli processing platform implementation has then been tested with Commercial Off-The-Shelf (COTS) to demonstrate the proof of concept.

Implementation and Experimental Setup

DBS and RS application impedance ranges (Fig. 2) are different: [2kΩ, 30kΩ] for the implanted DIXI DBS electrode and [20kΩ, 2MΩ] for the implanted retinal MEA. The shaping applied on stimuli is totally different from an application to another. The fit of each data set is performed with the "approximated" EEC using $C_{interface}$ instead of $Q_{interface}$ of Fig. 3. Values of EEC components are gathered in Table 1.

Data set	$R_{charge\text{-}transfer}$ (kΩ)	$C_{interface}$ (nF)	R_{bulk} (kΩ)	$C_{membrane}$ (pF)
Monkey (DBS)	269	533	1.9	289
Rat (RS)	1318	0.28	77.8	42

Table 1: EEC component values from EIS data fit.

To demonstrate the stimuli processing platform functionality, a voltage-mode signal generator is carried out in order to control stimulation targets voltage. Then, using the "approximated" EEC values and Matlab environment, each linear transfer function coefficients, linking $V_{STIM}(t)$ to $V_{TISSUE}(t)$, were estimated:

$$H_{DBS}(s) = \frac{0.9995s^2 + 0.7016s - 0.0007246}{s^2 + 970.35s - 1.001} \quad (3)$$

$$H_{RS}(s) = \frac{0.8518s^2 + 2319s - 0.04132}{s^2 + 5.794.10^4 s - 1.033} \quad (4)$$

The closed-loop system is implemented in Simulink environment. Its output signal $V_{STIM}(t)$ is extracted and sent into the voltage-mode signal generator (Agilent 33250A / 80MHz / 20Vpp). In this proof of concept, the electronic and biological noises were set to zero.

Results

A biphasic voltage waveform $V_{DEF\_TISSUE}(t)$ (phase duration=300µs, amplitude=1V, frequency=500Hz and interdelay=300µs) is defined as the variable set point for voltage in targets vicinity considering classical stimuli characteristics [3]. $V_{DEF\_TISSUE}(t)$ is computed into the stimuli processing platform for DBS and RS data. On Fig. 5, the adapted signal $V_{STIM}(t)$ (blue) is applied and $V_{TISSUE}(t)$ (green) is measured and compared to $V_{DEF\_TISSUE}(t)$ (red).

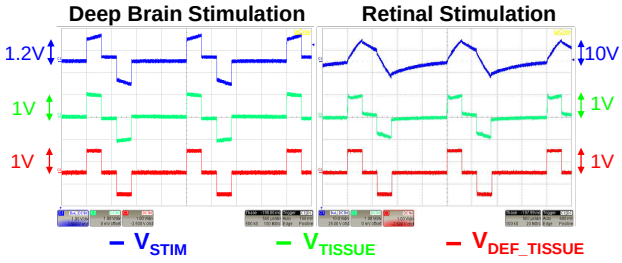

Fig. 5: Oscilloscope Lecroy (64MXs-A) screen prints of DBS (upper) and RS (lower) application custom waveform test.

As expected with the linear EEC test, in both cases, $V_{TISSUE}(t)$ is highly correlated to $V_{DEF\_TISSUE}(t)$. Signals' variability is discussed in the next section.

The signal $V_{STIM\_DBS}(t)$ magnitude (1.2V) is similar to $V_{DEF\_TISSUE}(t)$ magnitude (1V) and the signal shape is nearly identical. The signal $V_{STIM\_RS}(t)$ magnitude is about ten times $V_{DEF\_TISSUE}(t)$ magnitude and its shape is completely different from the initial biphasic square signal. Thereby, $V_{STIM}(t)$ adaptation seems more relevant for small electrode applications.

Discussion

The error observed between both $V_{TISSUE}(t)$ and $V_{DEF\_TISSUE}(t)$ is mainly due to the oscilloscope input capacitor C_{IN} (Fig. 6).

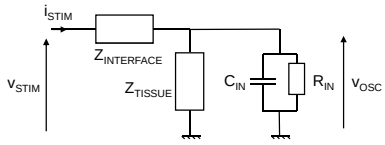

Fig. 6: Oscilloscope measurement principle schema.

C_{IN} (16pF) is interfering with the measurement. The resulting high-frequency filtering is more visible for $V_{TISSUE\_RS}(t)$ because $C_{membrane\_RS} < C_{membrane\_DBS}$ (42pF and 289pF respectively). $V_{STIM}(t)$ magnitude differences are directly linked to H low-frequency (LF) characteristics. Indeed, at 500Hz, H_{DBS}=0.95 and H_{RS}=0.05.

Our next aim is to test this platform for electrodes immersed in a physiological solution such as PBS (Phosphate Buffer Solution) and thereafter, for real *in vivo* conditions. Although the stimuli processing platform is operational with EEC, it might need improvements for further experiments. Certainly, the EIS measurements were performed at low voltage, in the impedance linearity range and far from electrical stimulation levels.

Impedance non-linearity toward voltage is highlighted on Fig. 7 when the voltage is increased from $20mV_{pp}$ to $4V_{pp}$, the LF capacitive behaviour starts to fade over 500mVpp (i.e. that the LF modulus decreases as the LF phase increases). Therefore, 20mVpp EIS measurements are necessarily linear. However, the stimulation levels, generally over $1V_{pp}$, might reach the non-linearity range impacting impedance levels as well as its shaping. Our stimulus adaption platform will yet stay relevant considering the electrode size reduction tendency leading to higher impedances and stronger shaping.

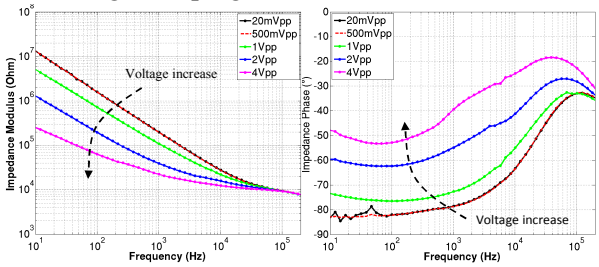

Fig. 7 : EIS performed on a MEA immersed in PBS for the voltage range [$20mV_{pp}$, $4V_{pp}$].

Different approaches might reinforce this method: the definition of a non-linear EEC model, the use of high-voltage EIS to approximate impedance non-linearity contributions or an online closed-loop control build around the actual electrode-tissue system. In this latter solution, the tracking system could refine iteratively the stimulus transmitted to the tissue.

Nowadays, few studies have been conducted on stimulation waveform clinical efficiency. In this study, it was showed that the effective waveform seen by the target is depending on the electrode size and layout. As each application implies specific electrodes, we can expect that controlling the stimulation waveforms at the target proximity opens the way for the development of stimulation devices more suited to each application.

Conclusions

We stated that for implanted devices, electrical stimuli are likely shaped by the electrode-tissue impedance and so, without EIS monitoring, this filtering is impossible to predict. This study proposed a stimuli processing platform addressing this issue. It was tested on EEC models deduced from DBS and RS applications and implemented with COTS. It is concluded from these results that this adaptation is possible whatever the application is, but remains more relevant when small electrodes are used due to their high impedance level. Further tests must be done in PBS and ultimately for *in vivo* conditions.

References

[1] J. J. Daly, E. B. Marsolais, L. M. Mendell, et al. Therapeutic neural effects of electrical stimulation. *IEEE Transactions on Rehabilitation Engineering*, vol. 4: pp. 218-230, 1996.

[2] A. L. Benabid. Deep brain stimulation for Parkinson's disease. *Current Opinion in Neurobiology*, vol. 13: pp. 696-706, 2003.

[3] D. R. Merrill, M. Bikson & J. G. R. Jefferys. Electrical stimulation of excitable tissue: design of efficacious and safe protocols. *Journal of Neuroscience Methods*, vol. 141: pp. 171-98, 2005.

[4] J. T. Wilson, W. Cui, X. L Sun, et al. In vivo biocompatibility and stability of a substrate-supported polymerizable membrane-mimetic film. *Biomaterials*, vol. 28: pp. 609-617, 2007.

[5] D. C. Johnson, D. W. Repperger & C. C. Ho. Development of a spectrally matched TENS stimulation waveform. *Biomedical Engineering Conference,* pp. 137–139, 1996.

[6] E. T. McAdams & J. Jossinet. Problems in equivalent circuit modelling of the electrical properties of biological tissue. *Bioelectrochemistry and Bioenergetics*, vol. 40: pp. 147-152, 1996.

[7] T. Ragheb & L. A. Geddes. Electrical properties of metallic electrodes. *Medical & Biological Engineering & Computing*, vol.28: pp.182-6, 1990.

[8] K. R. Cooper & M. Smith, "Electrical test methods for on-line fuel cell ohmic resistance measurement" *Journal of Power Sources*, vol. 160: pp. 1088-95, 2006.

[9] E. T. McAdams & J. Jossinet. Non-linear transient response of electrode-electrolyte interfaces. *IEEE Engineering in Medicine and Biology*, vol. 4: pp. 1789-1790, 1998.

[10] G. Chengwei & J. Qian. Optimized Proportional-Integral-Derivative Control Strategies and Simulation for Lower Limb Functional Electrical Stimulation. *International Conference on Information and Computing,* pp. 420-423, 2011.

Acknowledgements

The authors would like to thank F. Sauter (CEA) for the retinal MEA lending, the INT team (F. Chavane, S. Roux & F .Matonti) and the GIN team (O. David, N. Chivoret, B. Piallat & S. Charbardès) for respectively rat and monkey implantations.

Author's Address

Florent Dupont
PhD Student
florent.dupont@cea.fr